Desalination and Water Treatment
www.deswater.com

doi: 10.1080/19443994.2013.816873

52 (2014) 6549–6555
October

Taylor & Francis
Taylor & Francis Group

Kinetics and equilibrium studies on the electrosorption of anions with activated carbon electrodes

Limin Chang[a,*], Ying Zhou[a], Xiaoyue Duan[b]

[a]*School of Chemistry, Jilin Normal University, Siping 136000, China*
Tel. +86 434 3292094; Fax: +86 434 3292233; email: changlimin2139@163.com
[b]*School of Environmental Science and Engineering, Jilin Normal University, Siping, China*

Received 9 March 2013; Accepted 10 June 2013

ABSTRACT

In this paper, we prepared activated carbon (AC) electrodes with AC powder and self-made binder. The surface characteristics of AC electrode were characterized using scan electron microscope, contact angles of droplets, and N_2 adsorption–desorption isotherms. The results showed that the AC electrode had favorable hydrophilic property and high specific surface area ($717\,m^2\,g^-$). In addition, the electrosorption kinetics and isotherm of different anions (Cl^-, NO_3^-, SO_4^{2-}, CO_3^{2-} and PO_4^{3-}) on AC electrodes were investigated. The electrosorption of Cl^-, NO_3^-, SO_4^{2-}, CO_3^{2-} and, PO_4^{3-} on AC electrodes followed pseudo-first-order kinetics model; the monovalent ion (Cl^- and NO_3^-) had higher electrosorption capacity and electrosorption rate than multivalent ions (SO_4^{2-}, CO_3^{2-} and PO_4^{3-}), and Freundlich isotherm fitted electrosorption data of monovalent ions while the Langmuir isotherm fitted the experimental data of multivalent ions.

Keywords: Activated carbon electrode; Electrosorption; Anion; Kinetics; Isotherm

1. Introduction

Nowadays, seawater desalination has been considered as an effective method to solve the shortage of water resource [1]. Electrosorption, or referred to capacitive deionization (CDI), is a novel water desalination technology [2]. This electrochemical process is defined as potential-induced sorption on the surface of electrodes [3]. When an electrical potential is applied to the electrodes, charged ions in the solution are forced to move toward the opposite-charged electrodes by the electrostatic interactions [4], and then ions are held in the electrical double layers of electrodes. Thus, the ions are removed from the solution. Once the electric field is removed, the ions are quickly released back into the bulk solution [5], and the electrodes are regenerated. Compared with other traditional desalination methods such as reverse osmosis, thermal processes, and ion exchange, electrosorption desalination has several advantages: low-cost, long life cycle, easy regeneration, energy conservation, and without secondary pollution [5,6].

It is well known that the material of electrode is a key factor in electrosorption, so most research has been focused on the electrode material. According to the results shown in previous research, the activated carbon (AC) has large specific surface, and it is an ideal electrode material [7–9]. However, AC is a material that needs to be impregnated onto a substrate to

---

*Corresponding author.

make the AC electrode. Therefore, the binder is necessary. As is well known, most binders are hard after solidification and their wettability is very poor. The poor wettability is unfavorable for the electrosorption process, because it may take a long time before the ions in solution reach the interior of the electrodes. In order to obtain the AC electrodes with good wettability, we synthesized binder; and the AC electrodes were prepared with this binder. The morphology, wettability, and specific surface area of AC electrode were investigated using scan electron microscope (SEM), contact angle of water droplet, and N_2 adsorption–desorption isotherms. Besides, to obtain the electrosorption rate and electrosorption capacity of anions with different valences and sizes, the electrosorption experiments of NaCl, $NaNO_3$, Na_2SO_4, Na_2CO_3, and Na_3PO_4 were conducted under 1.2 V.

2. Materials and methods

2.1. Materials

AC powder and acrylic acid were purchased from Sinopharm Chemical Reagent Co. Ltd. (China). Azodiisobutyronitrile and tetraethylene glycol were supplied by Shanghai No. 4 Reagent & H.V. Chemical Co. Ltd. (China) and A Johnson Matthey Co. (Britain), respectively. All the reagents were of analytical grades and were used as received from the supplies without further purification.

2.2. Synthesis of binder

Into 250 mL of acrylic acid solvent (8.45 wt.%), 0.5 g of azodiisobutyronitrile was added. Then, the mixture was stirred at 70℃ for 3 h to form transparent and adhesive liquid. The binder was obtained after naturally cooling down to the room temperature.

2.3. Preparation and characterization of electrodes

In order to remove the soluble substance and other impurities, AC powder was firstly pretreated in boiling deionized water for 2 h, and washed with deionized water thoroughly, then dried at 110℃ for 24 h. AC electrode was prepared by mixing binder and pretreated AC powder in a weight ratio of 65:35 (the total weight was 1.0 g), where 6.5 mg tetraethylene glycol, as a firming agent, was added. The mixture was fully stirred and uniformly spread on a piece of graphite paper (as a current collector), then dried at 120℃ for 20 min. Finally, the samples were carbonized at 850℃ for 1 h in nitrogen atmosphere. After naturally cooling down to ambient temperature, the carbonized AC electrodes were obtained. All the electrodes were 5 cm in length, 2.6 cm in width, and about 1 mm in thickness. Carbon nanotube (CNT) electrode was prepared following the same method of AC electrode, only replacing AC with CNT. Activated carbon fiber (ACF) electrode was obtained by cutting ACF cloth into 2.6×5 cm in area (weight 0.17 g) and connecting it on the graphite paper with string.

The morphology of AC electrode was characterized with digital camera (Sony) and scan electron microscope (SEM, S-570, Hitachi). The contact angle of water droplet on the electrode was tested by the contact angle goniometer (JC2000CD, Powereach). The Brunauer–Emmett–Teller (BET) specific surface area, pore size distribution, and the pore volume of AC electrode were analyzed by N_2 adsorption–desorption isotherms on a Micromeritics 3H-2000PS1 instrument.

2.4. Electrosorption measurements

Batch-mode electrosorption experiments were conducted in a cell with a dimension of 5 cm (length) × 1.6 cm (width) × 3 cm (height). All experiments were conducted using 20 mL of 2 $\mathrm{mmol\,L^{-1}}$ salt solutions (NaCl, $NaNO_3$, Na_2SO_4, Na_2CO_3 and Na_3PO_4) made up in deionized water. The electrodes were placed face to face at both sides with a distance of 1.5 cm and connected with a DC power supply. The DC power supply maintained a constant voltage of 1.2 V during electrosorption process. In our experiments, all the electrodes were fresh materials. The salt concentrations were measured with a DDS-11A conductivity meter, and the corresponding concentration can be obtained with a calibration curve made prior to the experiments.

In the experiments, the electrosorption capacity ($\mathrm{mmol\,g^{-1}}$) can be defined as follows:

$$\text{Electrosorption capacity} = \frac{(C_0 - C_e) \times V}{m} \tag{1}$$

where C_0 and C_e are the initial and equilibrium concentrations ($\mathrm{mmol\,L^{-1}}$), respectively, V is the volume of solution (L), and m is the mass of carbon material.

The desorption efficiency was calculated according to the following equation:

$$\eta = \left(\frac{C_f - C_e}{C_0 - C_e}\right) \times 100\% \tag{2}$$

where C_f is the final concentrations ($\mathrm{mmol\,L^{-1}}$) after desorption.

3. Result and discussion

3.1. Characteristics of AC electrodes

Digital picture and SEM image of AC electrode are presented in Fig. 1(a), (b). It can be seen in Fig. 1(a) that there are many fine and homogeneous cracks on AC electrode which were formed during the process of carbonization treatment. These cracks greatly improved the flexibility of AC electrode. The flexibility is one of the characteristics the good AC electrode should have. If the AC electrode lacks flexibility, the AC on the electrode tends to fall off in a big piece due to local force when it is cut into desired size and it is hard to stack the AC electrodes in building a CDI assembly. In addition, these cracks can help the solution reach the interior of the electrodes in a shorter time. In Fig. 1(b), it can be seen that the AC was not covered by the binder. Thus, we deduced that the self-made binder would not cause the decrease of surface area AC or bad wettability of electrode, which is beneficial for the electrosorption of AC electrode.

The contact angle of water droplet on the electrode is the important way to evaluate the wettability of electrode, so the contact angles of water droplet on the surface of AC electrode were tested every 0.4 s. Fig. 2 shows the contact angle images of water droplet on the AC electrode. As shown in Fig. 2(a), after 0.8 s, the water droplet was absorbed completely and the water drop on the electrode could not be captured, which confirmed the deduction in SEM that the self-made binder would not cause bad wettability of AC electrode; that is, the AC electrode prepared in this work had an excellent hydrophilicity.

It is well known that, pore structure, pore size, and surface area of porous electrodes affect their electrosorption performance. Thus, the BET area and pore distribution of AC electrode was tested. The BET surface area was $717\,m^2\,g^{-1}$, the total pore volume was $0.5306\,cm^3\,g^{-1}$, and the average pore diameter was calculated to be around 2.96 nm. Fig. 3 shows the N_2 adsorption/desorption isotherms and BJH pore size distribution plots of AC. Typical type-IV isotherms with a hysteresis loop between the adsorption and desorption branches can be seen in Fig. 3(a), indicating existence of mesopores. This also can be seen in the pore size distribution analysis in Fig. 3(b). It also can be seen in Fig. 3(b) that the pore distribution is no smaller than 1 nm and no bigger than 50 nm, which is beneficial to electrosorption.

The electrosorption capacity and desorption ratio of AC electrode were compared with those of ACF and CNT electrodes. Table 1 lists the electrosorption capacity and desorption ratios of different electrode materials. As can be seen from Table 1, the electrosorption capacity of AC electrode is $0.049\,mmol\,g^{-1}$, which is lower than those of ACF and CNT electrodes. However, it is higher than the electrosorption capacity of AC sheet in literature. Hou et al. prepared AC sheet electrode with polyvinylidene fluoride binder; under the same electrosorption experimental conditions, the electrosorption capacity for $2\,mmol\,L^{-1}$ NaCl solution was $0.0423\,mmol\,g^{-1}$. Even treatment in 1 M KOH solution, the electrosorption capacity of NaCl on their AC sheet was $0.0445\,mmol\,g^{-1}$, which is still lower than that of AC electrode prepared in this study [3]. In addition, it also can be seen in Table 1 that the desorption ratio of AC electrode is higher than those of ACF and CNT electrodes, indicating that the AC electrode has better regeneration charateristics. Besides, considering the price of these carbon materials, the price of AC is far less than those of ACF and CNT; it is best suitable for the preparation of

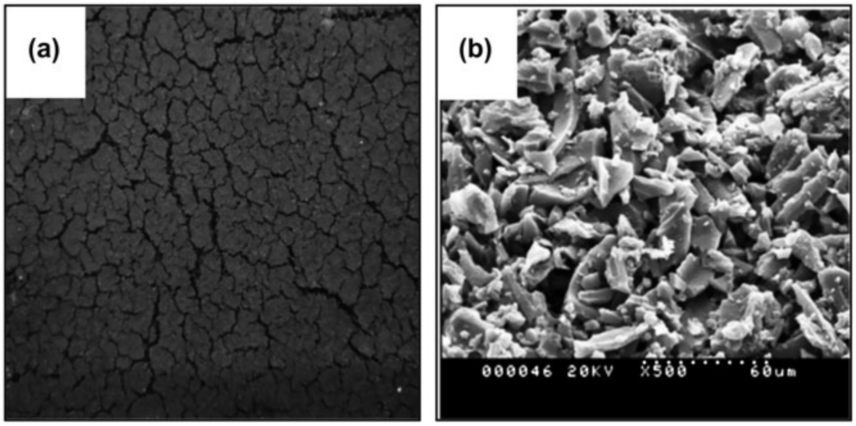

Fig. 1. Digital picture (a) and SEM image (b) of AC electrode.

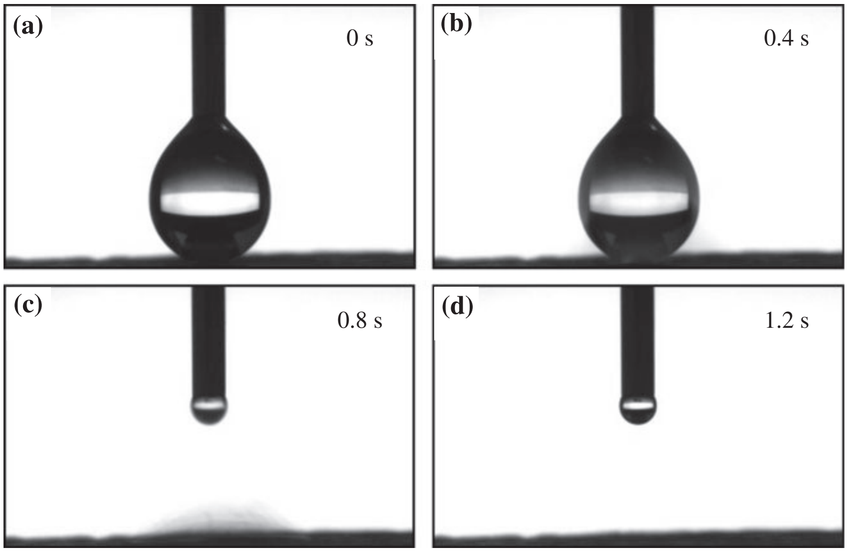

Fig. 2. Contact angle images of water droplet on AC electrode.

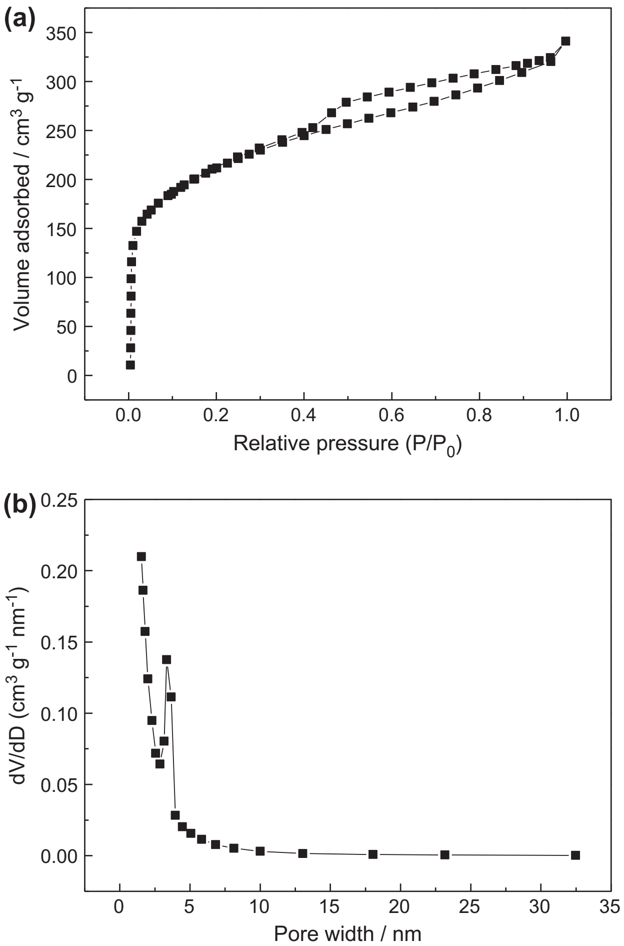

Fig. 3. Nitrogen sorption isotherms (a) and pore size distribution curves (b) of AC electrode.

electrodes in large scale. So, it could be concluded that AC electrode will be promising in the electrosorption desalination industry.

3.2. Electrosorption kinetics and isotherms

The typical electrosorption experiments were conducted in 20 mL salt solution with an initial concentration of $2\,\text{mmol}\,\text{L}^{-}$ to understand the electrosorption and desorption processes of different anions. Fig. 4 is the curves of electrosorption and desorption of Cl^{-}, NO_3^{-}, SO_4^{2-}, CO_3^{2-}, and PO_4^{3-}. Under potential of 1.2 V, the concentration of ions decreased sharply during the first 60 min, and then the concentration decreased slowly. When the adsorption times were about 180, 180, 180, 185, and 160 min, respectively, for Cl^{-}, NO_3^{-}, SO_4^{2-}, CO_3^{2-}, and PO_4^{3-}, the concentrations of anions no longer decreased and the electrosorption reached equilibrium for each anion. The removal ratios of Cl^{-}, NO_3^{-}, SO_4^{2-}, CO_3^{2-} and PO_4^{3-} at adsorption equilibrium were 80.2, 80.0, 76.3, 70.3, and 40.8%, respectively. When applying an opposite potential of −1.2 V, the ions absorbed on the electrodes was repulsed by the electrodes, and released into the solution. Therefore, the electrosorption process is a reversible process, and the AC electrodes can be regenerated by applying an opposite potential on electrodes. However, it can be seen that the desorption ratio of different anions was not consistent; their desorption ratio decreased in the same order as the electrosorption ratio: $\text{Cl}^{-} > \text{NO}_3^{-} > \text{SO}_4^{2-} > \text{CO}_3^{2-} > \text{PO}_4^{3-}$. The discrepancy of desorption ratios of different anions might be

Table 1
Comparison of different electrodes

Kind of electrode	Adsorption capacity (mmol g^{-1})	Desorption ratio (%)
AC	0.049	87.23
ACF	0.061	73.65
CNT	0.073	61.96

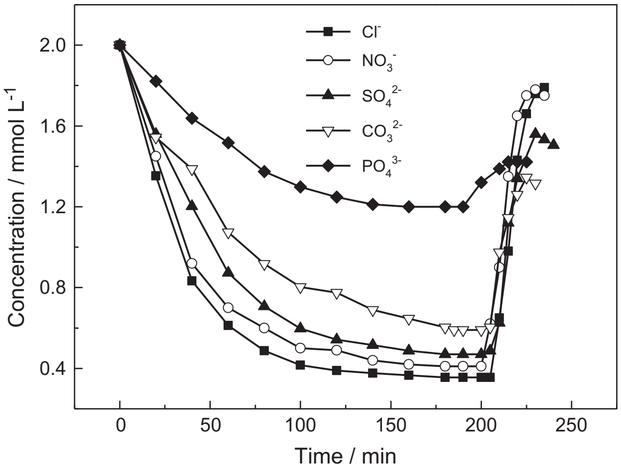

Fig. 4. The electrosorption and desorption curves of Cl^-, NO_3^-, SO_4^{2-}, CO_3^{2-}, and PO_4^{3-} on AC electrodes.

associated with their different physical adsorption removal ratios on AC electrodes. In order to determine the physical adsorption removal ratios of different anions, the adsorption process was carried out at open circuit condition for 180 min. The result was that the physical adsorption removal ratios were 1.2, 8.0, 5.4, 21.3, and 36.9%, respectively, for Cl^-, NO_3^-, SO_4^{2-}, CO_3^{2-}, and PO_4^{3-}. When comparing the physical adsorption removal ratios with desorption ratios, it was found that the higher the physical adsorption removal ratio of anion, the lower the desorption ratio, which indicated that the anions adsorbed on AC resulted by physical adsorption is hard to desorb.

To understand the electrosorption rate and electrosorption capacity of anions on AC electrodes, the pseudo-first-order model equation was employed to fit experimental data. The form of the model equation can be formulated as [10]:

$$\log(q_e - q) = \log q_e - \frac{kt}{2.303} \tag{3}$$

where k is the pseudo-first-order adsorption rate constant (min^{-1}) and, q_e and q are the amounts of adsorbed salt at equilibrium and time t (min), respectively. The results shown in Fig. 5 and Table 2 suggest that the pseudo-first-order kinetics equation can fit the experimental data due to the high value of the correlation coefficient (R^2). The results also show that the monovalent ion (Cl^- and NO_3^-) had higher electrosorption capacity and rate than multivalent ions (SO_4^{2-}, CO_3^{2-} and PO_4^{3-}). This result could be associated with the hydrated radius of these anions (listed in Table 3), which is a function of charge and ionic radius (i.e. charge-to-radius ratio) [2]. The anions with smaller hydrated radius might occupy smaller surface area of AC electrode, and had the higher electrosorption capacity. So, monovalent ions with smaller hydrated radius showed higher removal efficiency than the multivalent ions with bigger hydrated radius.

To further compare electrosorption behavior of Cl^-, NO_3^-, SO_4^{2-}, CO_3^{2-}, and PO_4^{3-} on AC electrodes, the batch experiments at different temperatures were carried out under the bias potential of 1.2 V. Langmuir isotherm (Eq. (4) and Freundlich isotherm (Eq. (5) [1,13,14] were used to fit the experimental data for Cl^-, NO_3^-, SO_4^{2-}, CO_3^{2-}, and PO_4^{3-} adsorption on AC electrodes.

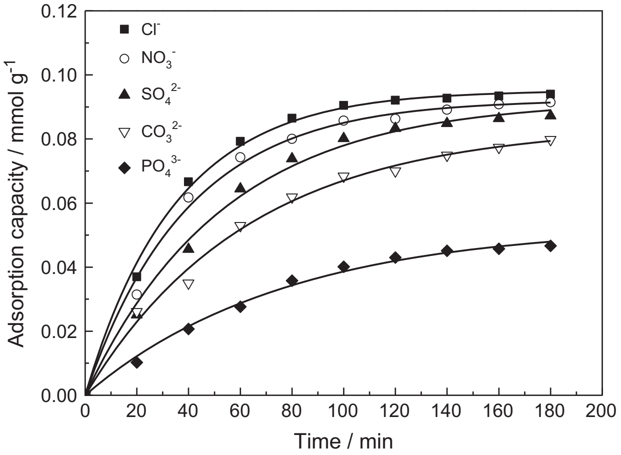

Fig. 5. The electrosorption kinetics of Cl^-, NO_3^-, SO_4^{2-}, CO_3^{2-}, and PO_4^{3-} on AC electrodes.

Table 2
The electrosorption parameters of first-order adsorption kinetics for Cl^-, NO_3^-, SO_4^{2-}, CO_3^{2-}, and PO_4^{3-} on AC electrodes

Anions	q_e ($\times 10^{-2}$ mmol g^{-1})	k ($\times 10^{-2}$ min^{-1})	R^2
Cl^-	9.50	2.80	0.9965
NO_3^-	9.24	2.53	0.9940
SO_4^{2-}	9.22	1.87	0.9941
CO_3^{2-}	8.42	1.59	0.9930
PO_4^{3-}	5.31	1.30	0.9936

Table 3
Chemical data of test ions [11–12]

Anions	Charge	Hydrated radius (pm)
Cl^-	−1	332
NO_3^-	−1	335
SO_4^{2-}	−2	379
CO_3^{2-}	−2	394
PO_4^{3-}	−3	400

$$q_e = \frac{q_m K_L c_e}{1 + K_L c_e} \tag{4}$$

$$q_e = K_F c_e^{1/n} \tag{5}$$

where q_e is the amount of adsorbed salt at equilibrium (mmol g^{-1}), q_m is the maximum saturation adsorption capacity at the constant temperature (mmol g^{-1}), K_L is the Langmuir constant related to the energy of adsorption (L mmol^{-1}), c_e is the equilibrium concentration of adsorbate in solution (mmol L^{-1}), K_F is Freundlich constant related to the adsorption capacity of absorbent, and $1/n$ is the indication of the tendency of the adsorbate to be adsorbed.

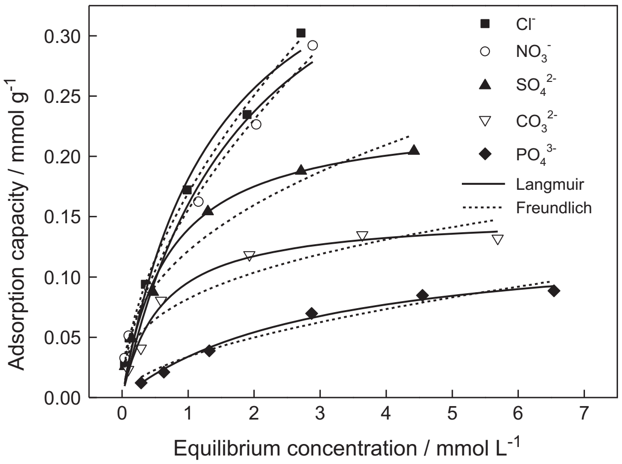

Fig. 6. The electrosorption isotherms of Cl^-, NO_3^-, SO_4^{2-}, CO_3^{2-}, and PO_4^{3-} at different temperatures.

Table 4
The isotherms parameters of Cl^-, NO_3^-, SO_4^{2-}, CO_3^{2-} and PO_4^{3-} electrosorption on AC electrodes at different temperatures

Anion	Langmuir			Freundlich		
	q_m	K_L	R^2	K_F	n	R^2
Cl^-	0.4388	0.7027	0.9757	0.1694	1.7695	0.9976
NO_3^-	0.3927	0.5389	0.9552	0.1556	1.7644	0.9929
SO_4^{2-}	0.2331	1.4558	0.9889	0.1215	2.5432	0.9637
CO_3^{2-}	0.1519	1.6910	0.9837	0.0819	2.9555	0.8860
PO_4^{3-}	0.1343	0.3375	0.9878	0.0338	1.7919	0.9484

Fig. 6 shows the adsorption isotherms, and the isotherm parameters obtained are summarized in Table 4. Based on the values of correlation coefficient (R^2), it was found that the experimental data of Cl^- and NO_3^- correlated better with Frendlich isotherm, those of SO_4^{2-}, CO_3^{2-}, and PO_4^{3-} correlated better with Langmuir isotherm. These results show that the Frendlich isotherm fitted the electrosorption data of monovalent ions, suggesting multilayer coverage of monovalent ions on AC during electrosorption, while the Langmuir isotherm fitted the electrosorption data of multivalent ions, suggesting monolayer coverage of multivalent ions on AC during electrosorption. By comparing the adsorption capacity of different anions, we can conclude that the multilayer coverage was more beneficial for electrosorptipn of anions on AC electrode than the monolayer coverage.

4. Conclusion

The AC electrodes were fabricated with AC powder and self-made binder. The AC electrodes had excellent hydrophilicity and high specific surface area. The electrosorption of different anions (Cl^-, NO_3^-, SO_4^{2-}, CO_3^{2-}, and PO_4^{3-}) with different valence and hydrated radius followed pseudo-first-order kinetics model and their electrosorption rate and capacity both decreased in the order $Cl^- > NO_3^- > SO_4^{2-} > CO_3^{2-} > PO_4^{3-}$. The results of adsorption isotherm fitting showed that Frendlich isotherm fitted electrosorption data of monovalent ions while the Langmuir isotherm fitted the experimental data of multivalent ions.

Acknowledgments

This project is supported financially by Science and Technology Ministry of Jilin Province, China (No. 20120407), and the Science and technology Project of Jilin Education Bureau, China (No. 20130209).

References

[1] Y. Zhan, C. Nie, H. Li, S. Sun, Kinetics and isotherm studies on electrosorption of NaCl by activated carbon fiber, carbon nanotube and carbon nanotube-carbon nanofiber composite film, Phys. Stat. Sol. C 9 (2012) 55–58.

[2] J. Gabelich Christopher, I.H. Tran Trid, "Mel" Suffet, Electrosorption of inorganic salts from aqueous solution using carbon aerogels, Environ. Sci. Technol. 36 (2002) 3010–3019.

[3] C.H. Hou, J.F. Huang, H.R. Lin, B.Y. Wang, Preparation of activated carbon sheet electrode assisted electrosorption process, J. Taiwan Inst. Chem. Eng. 43 (2012) 473–479.

[4] B.H. Park, Y.J. Kim, J.S. Park, J. Choi, Capacitive deionization using a carbon electrode prepared with water-soluble poly (vinyl alcohol) binder, J. Ind. Eng. Chem. 17 (2011) 717–722.

[5] H. Li, L. Pan, T. Lu, Y. Zhan, C. Nie, Z. Sun, A comparative study on electrosorptive behavior of carbon nanotubes and graphene for capacitive deionization, J. Electroanal. Chem. 653 (2011) 40–44.

[6] B. Jia, L. Zou, Graphene nanosheets reduced by a multi-step process as high-performance electrode material for capacitive deionization, Carbon 50 (2012) 2315–2321.

[7] R.L. Machunda, H. Jeon, J.K. Lee, J. Lee, Effects of acid treatment in the improvement of specific capacitance and deionization efficiency of porous carbon electrodes, Water Sci. Technol. Water Supply 9 (2009) 159–165.

[8] I. Villar, S. Roldan, V. Ruiz, M. Granda, C. Blanco, R. Menéndez, R. Santamaría, Capacitive deionization of NaCl solutions with modified activated carbon electrodes, Energ. Fuel 24 (2010) 3329–3333.

[9] Z. Chen, C. Song, X. Sun, H. Guo, G. Zhu, Kinetic and isotherm on the electrosorption of NaCl from aqueous solutions by activated carbon electrodes, Desalination 267 (2011) 239–243.

[10] S. Wang, D. Wang, L. Ji, Y. Zhu, J. Liang, Equilibrium and kinetic studies on the removal of NaCl from aqueous solutions by electrosorption on carbon nanotube electrodes, Sep. Purif. Technol. 58 (2007) 12–16.

[11] Department of Anlytical chemistry of Hangzhou University, Analytical Chemistry: Basic and Safety Knowledge, Chemical Industry Press, Beijing, 2003.

[12] E.R. Jr, Nightingale, phenomenological theory of ion salvation: Effetive radii of hydrated ions, J. Phys. Chem. 63 (1959) 1381–1387.

[13] S. Chatterjee, T. Chatterjee, S.R. Lim, S.H. Woo, Adsorption of a cationic dye, methylene blue, onto chitosan hydrogel beads generated by anionic surfactant gelation, Environ. Technol. 32 (2011) 1503–1514.

[14] N.M. Mahmoodi, B. Hayati, M. Arami, Kinetic, equilibrium and thermodynamic studies of ternary system dye removal using a biopolymer, Ind. Crops Prod. 35 (2012) 295–301.